Electronic Supplementary Material (ESI) for Materials Advances.

Synthesis and ionic conductivity of calcium doped ceria relevant to Solid oxide fuel cell applications

Momin et al.

Supplementary Information

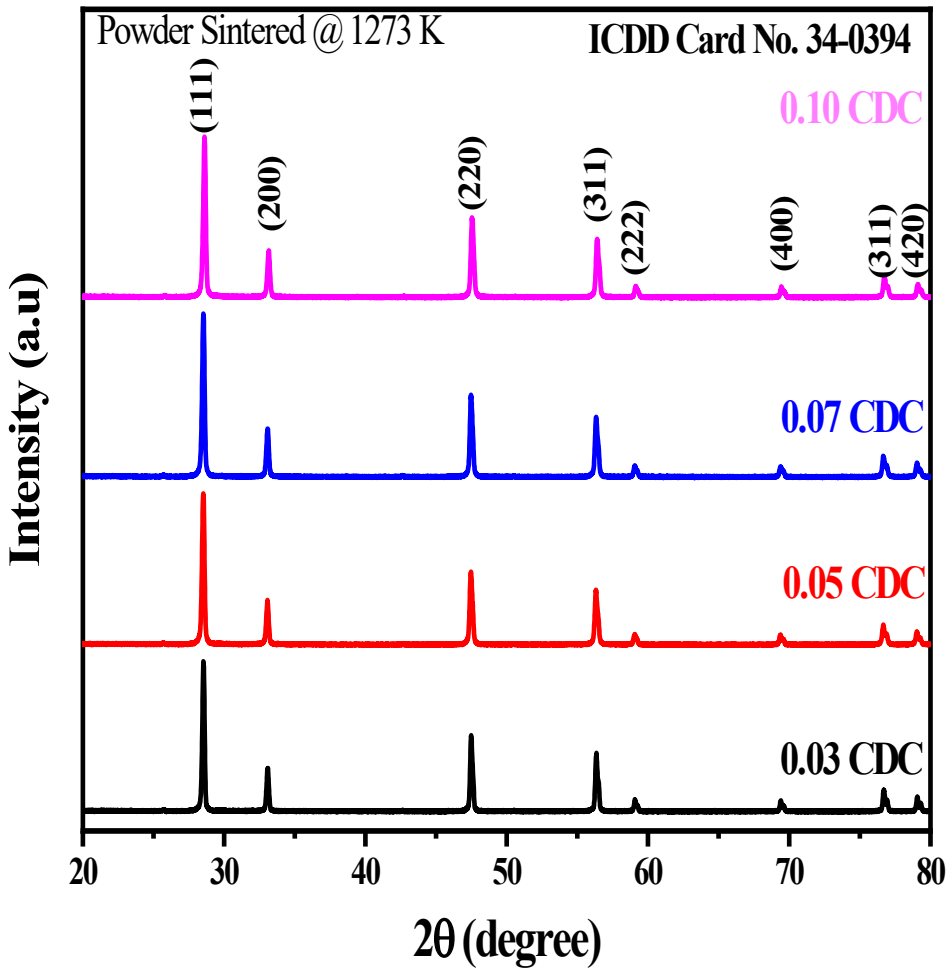

Fig. 1S XRD pattern of pellet CDC powder samples sintered at 1273 K.

The Rietveld refinement of CDC pellets have been performed using PROFEX software. From the obtained results it is clear that the difference between the calculated and observed XRD pattern is negligible. The refinement parameters are shown in Table 1S.

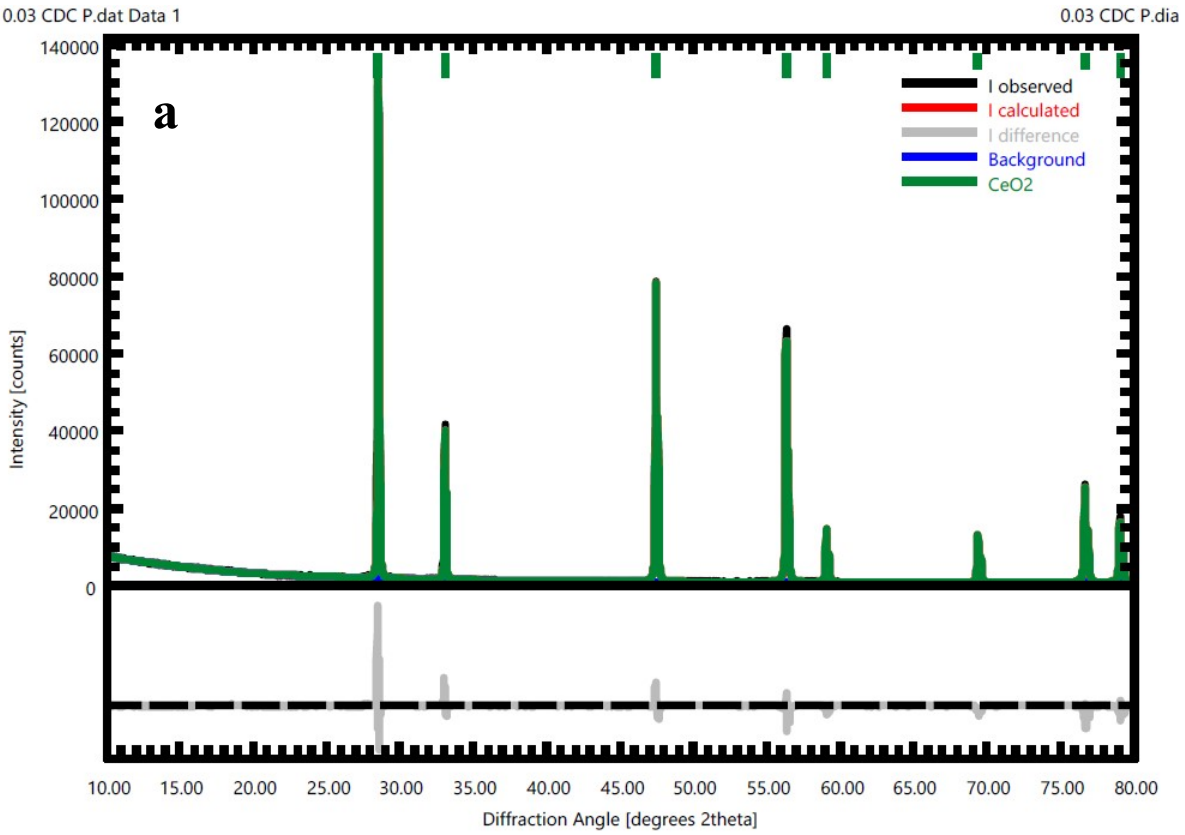
0.03 CDC P.dat Data 1
0.03 CDC P.dia
a
I observed
I calculated
I difference
Background
CeO2
Intensity [counts]
140000
120000
100000
80000
60000
40000
20000
0
10.00
15.00
20.00
25.00
30.00
35.00
40.00
45.00
50.00
55.00
60.00
65.00
70.00
75.00
80.00
Diffraction Angle [degrees 2theta]

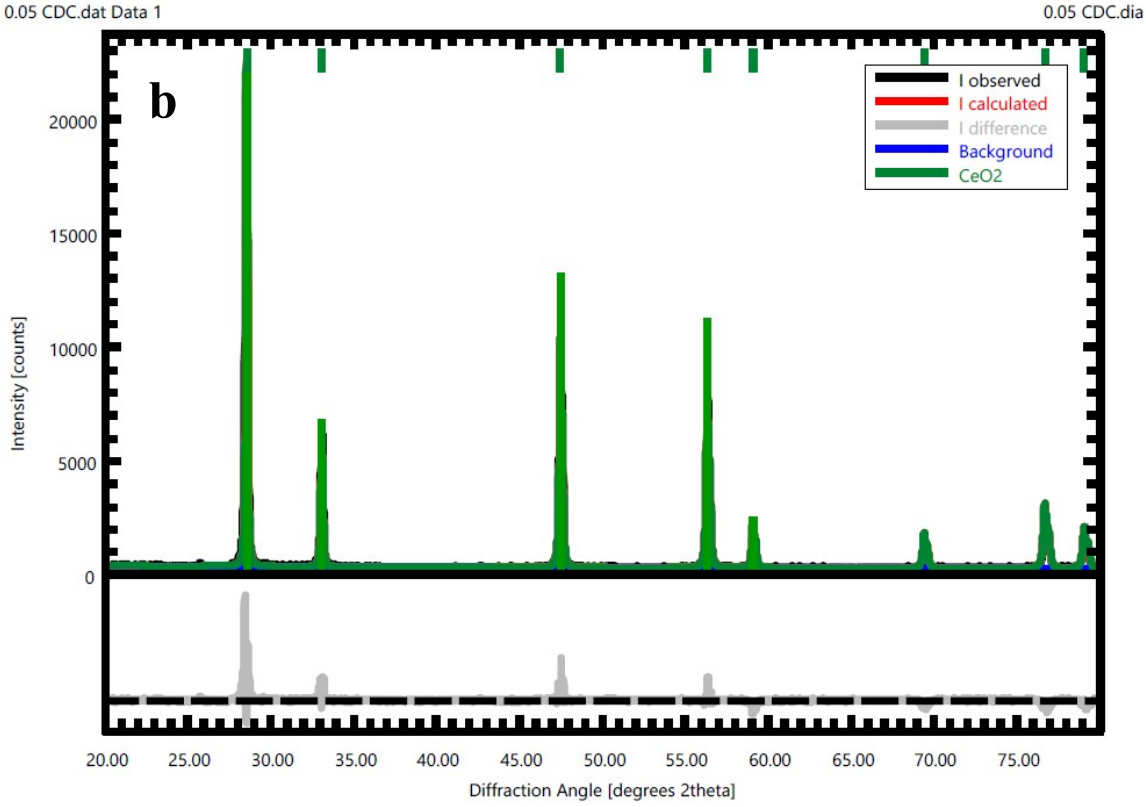
0.05 CDC.dat Data 1
0.05 CDC.dia
b
I observed
I calculated
I difference
Background
CeO2
Intensity [counts]
20000
15000
10000
5000
0
20.00
25.00
30.00
35.00
40.00
45.00
50.00
55.00
60.00
65.00
70.00
75.00
Diffraction Angle [degrees 2theta]

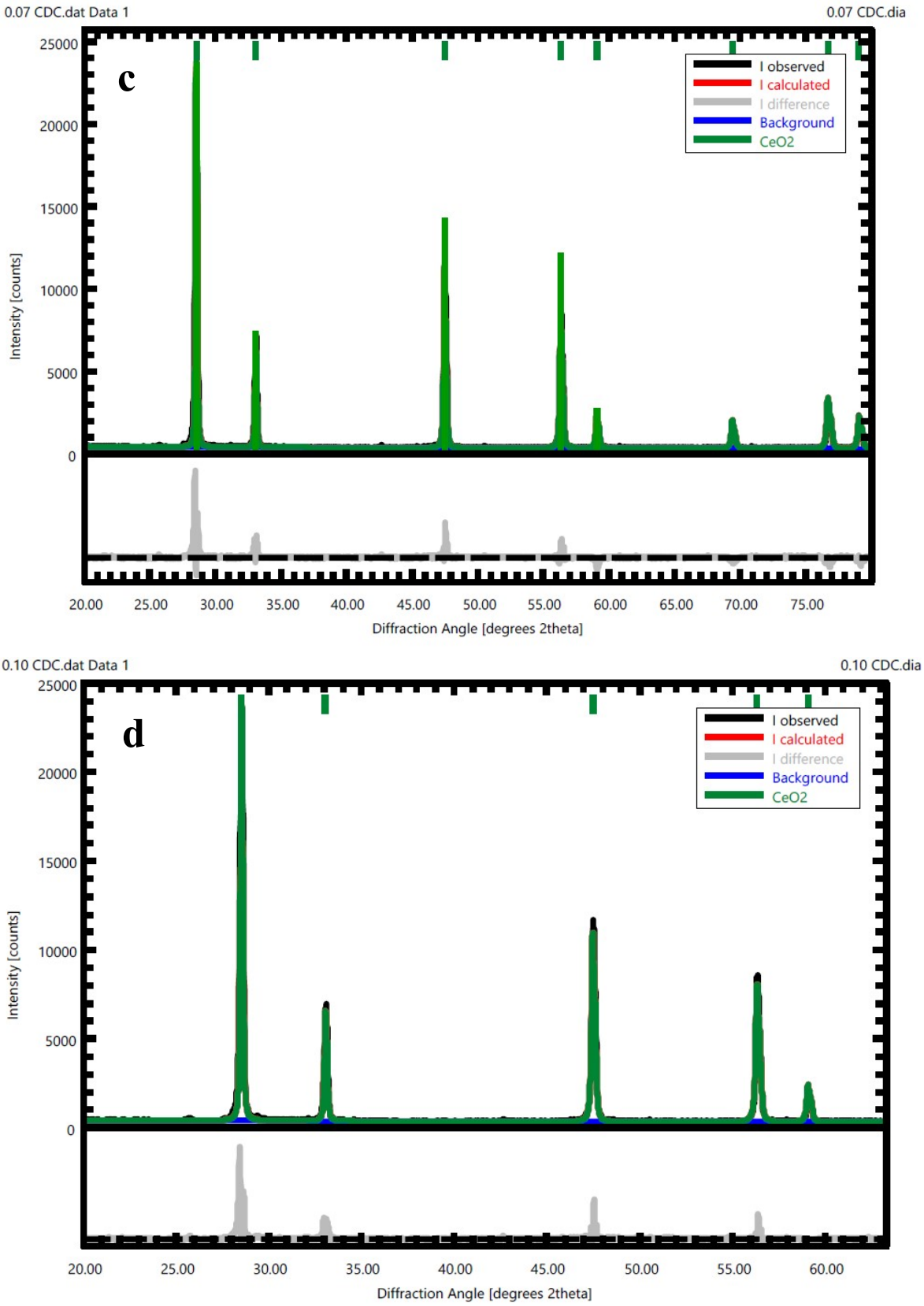

Fig. 2S XRD patterns after Rietveld refinement (a) 0.03, (b) 0.05, (c) 0.07 and (d) 0.10 CDC pellets.

Table 1S

Rietveld refinement parameters of CDC samples

Sample	Agreement factors			Average Crystallite Size in nm
	R_P	R_{wp}	GoF	
0.03 CDC	2.22	5.49	2.47	318
0.05 CDC	4.58	12.39	2.70	136
0.07 CDC	4.43	12.33	2.78	127
0.10 CDC	4.42	12.62	2.85	108

The FT-IR spectra of CDC samples is shown in Fig. 4S. The band at 3984 cm^{-1} represent the stretching mode of C–H bond and the bands 2911 cm^{-1} and 2853 cm^{-1} due to the organic molecules absorbed during synthesis [1-4]. The 3434 cm^{-1} and 1626 cm^{-1} bands are ascribed to (O–H) vibration modes of water (H–bonded) molecules [5]. The 1767 cm^{-1} band is due to stretching vibration of carboxylate salts (COO^{-}) and that at 1027 cm^{-1} is due to the cerium-oxygen [6]. The weaker band at 717 cm^{-1} is attributed to the Ce–O group having lower double bond nature and Ce–O–Ce chains of asymmetric stretching vibration of metal oxide. The stretching vibration band of Ce–O–Ca bonds is represented by the band at 887 cm^{-1} [7, 8].

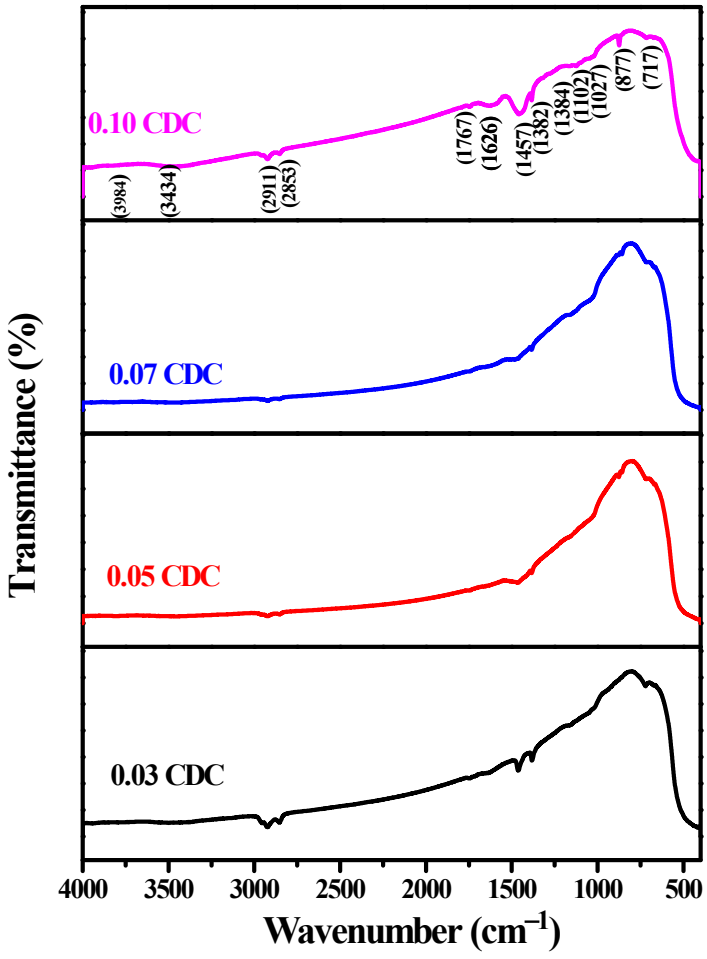

Fig. 3S FT-IR spectra of CDC samples.

The Kubelka– Munk plots of CDC samples for optical band gap are shown in **Fig. 4S.** It is found that, the band-gap energy decreased with increase in dopant (Ca) concentration (Table. 1), compared to the reported band-gap energy of 3.33 eV for cerium oxide [9]. The Ca ions are engendered at the ground and excited f-energy state in the CeO_2 band during the doping process. From the energy state of Ca entraps lots of excited electrons impending from O2−2p level and hence causing the decrease in bandgap energy [10]. The values for the energy bandgap determined from the Kubelka– Munk plots decrease from 3.33 for CeO_2 to 2.98, 2.88, 2.82 to 2.80 eV for 0.03 CDC, 0.05 CDC, 0.07 CDC and 0.10 CDC respectively.

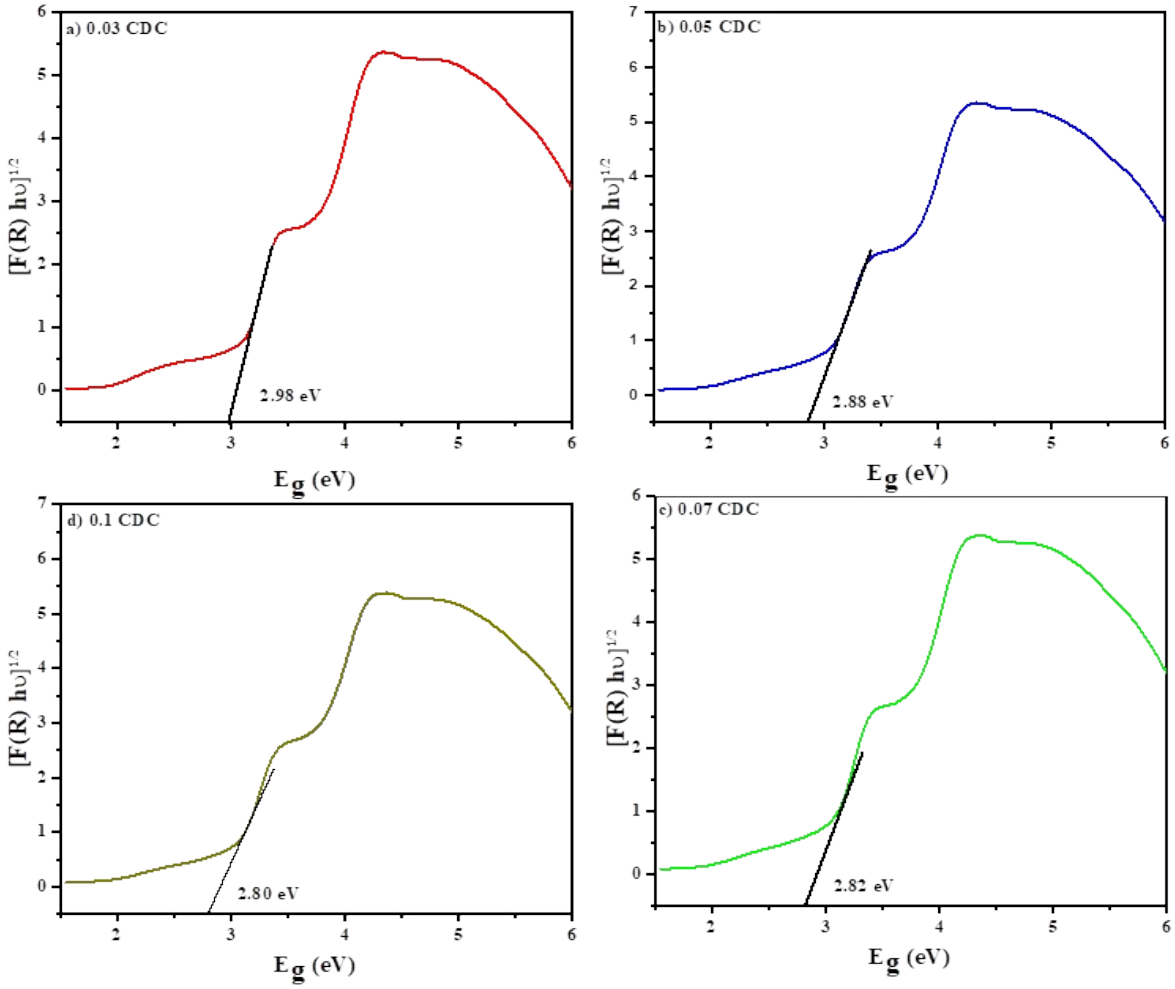

Fig. 4S Kubelka–Munk plots of CDC samples.

(a) 0.03 CDC

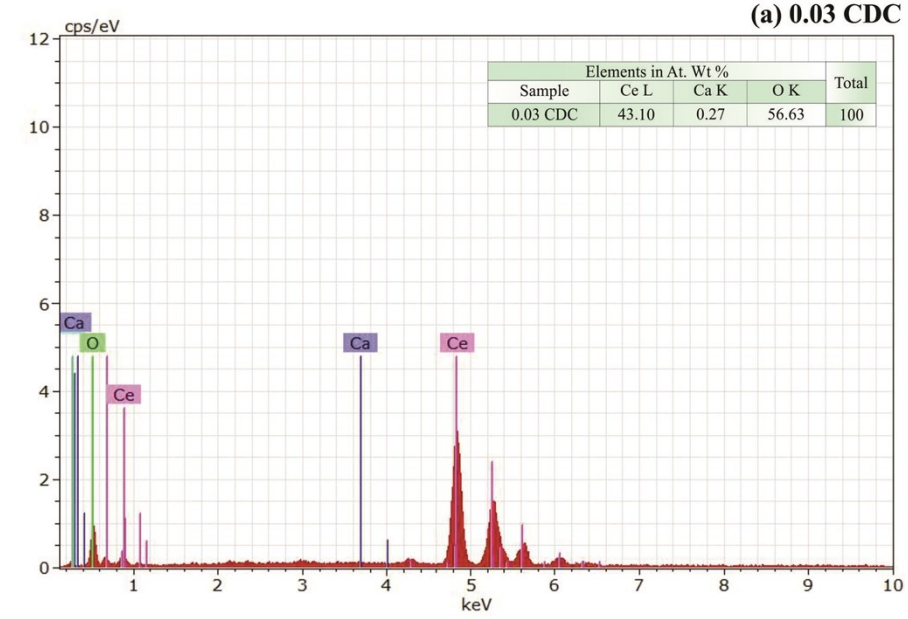

Elements in At. Wt %				Total
Sample	Ce L	Ca K	O K	
0.03 CDC	43.10	0.27	56.63	100

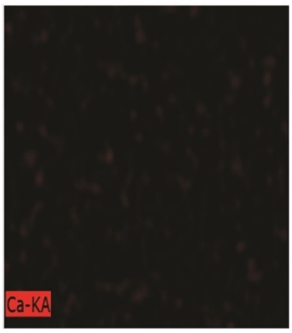

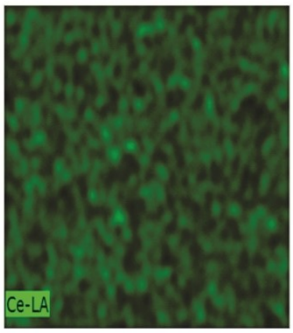

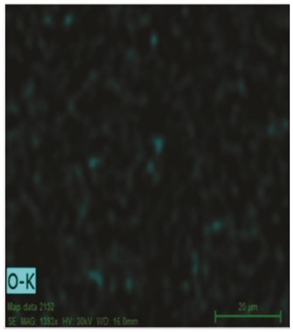

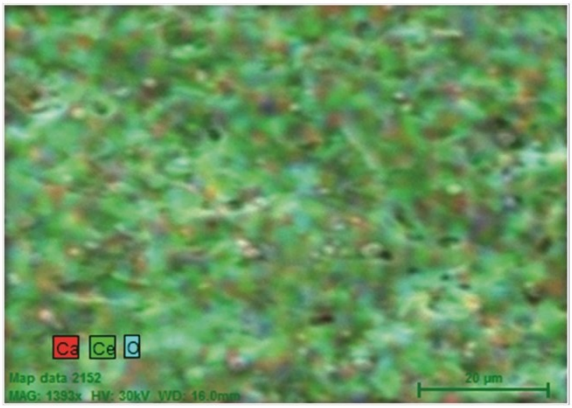

(b) 0.05 CDC

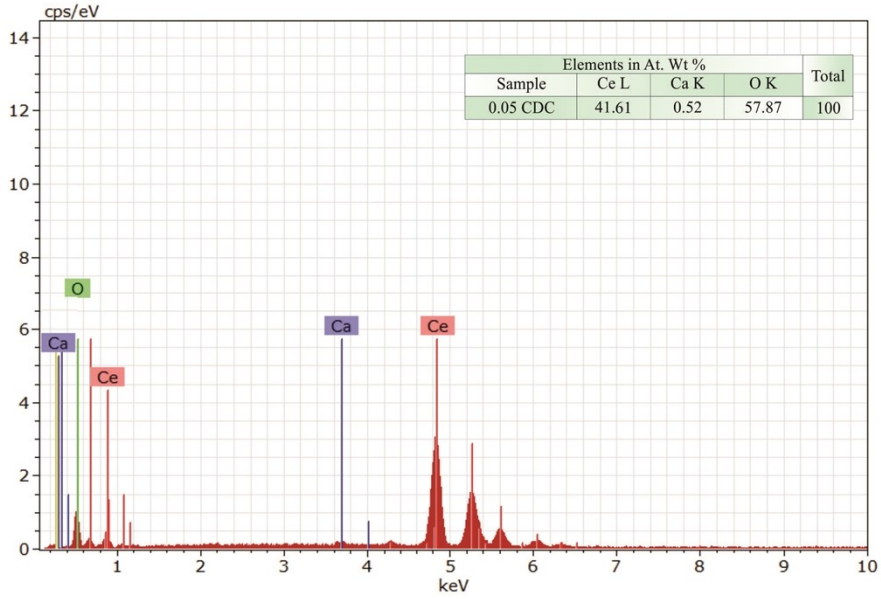

Elements in At. Wt %				Total
Sample	Ce L	Ca K	O K	
0.05 CDC	41.61	0.52	57.87	100

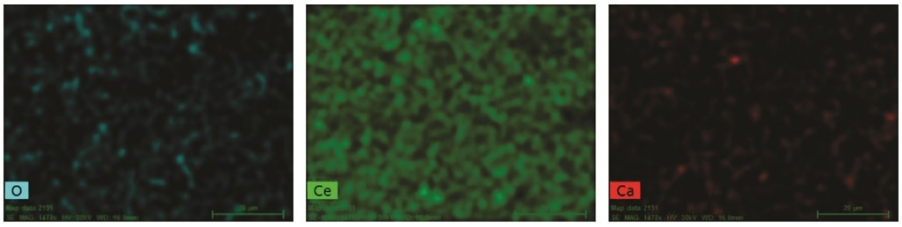

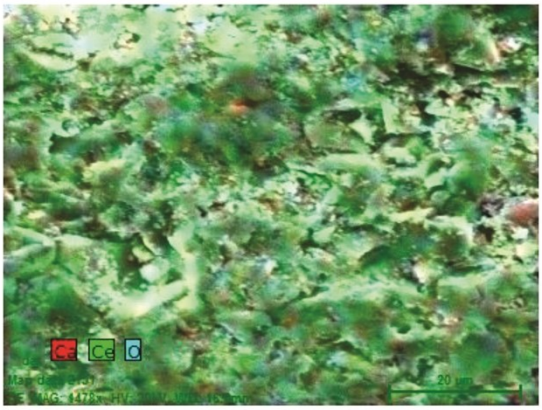

(c) 0.07 CDC

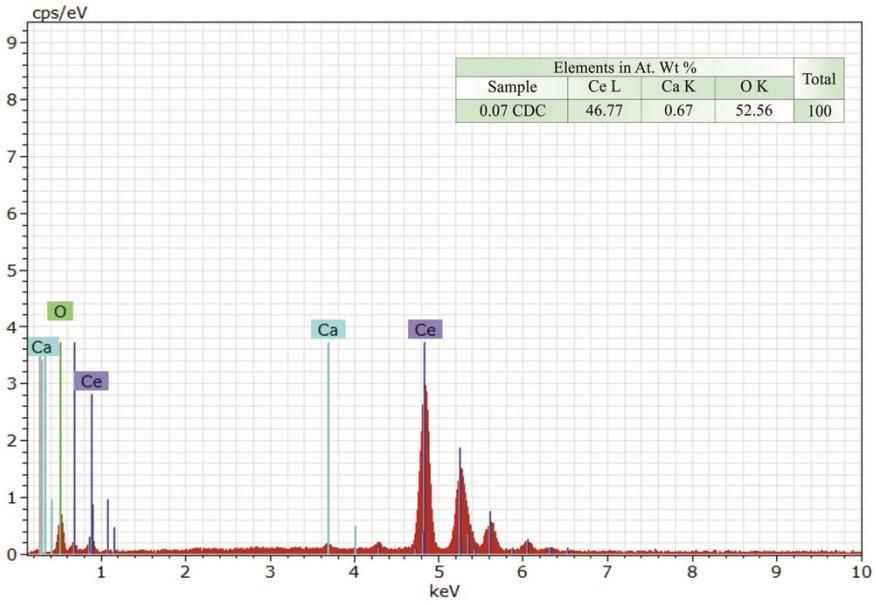

Elements in At. Wt %				Total
Sample	Ce L	Ca K	O K	
0.07 CDC	46.77	0.67	52.56	100

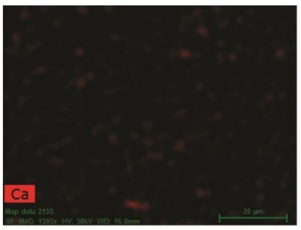

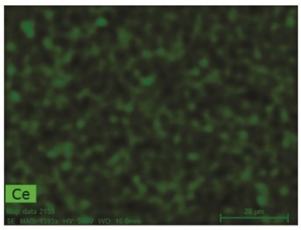

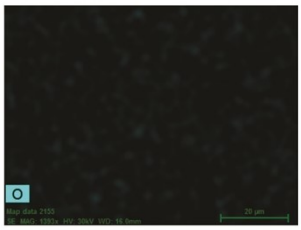

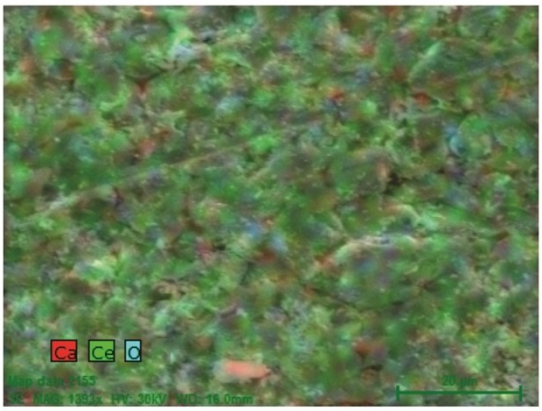

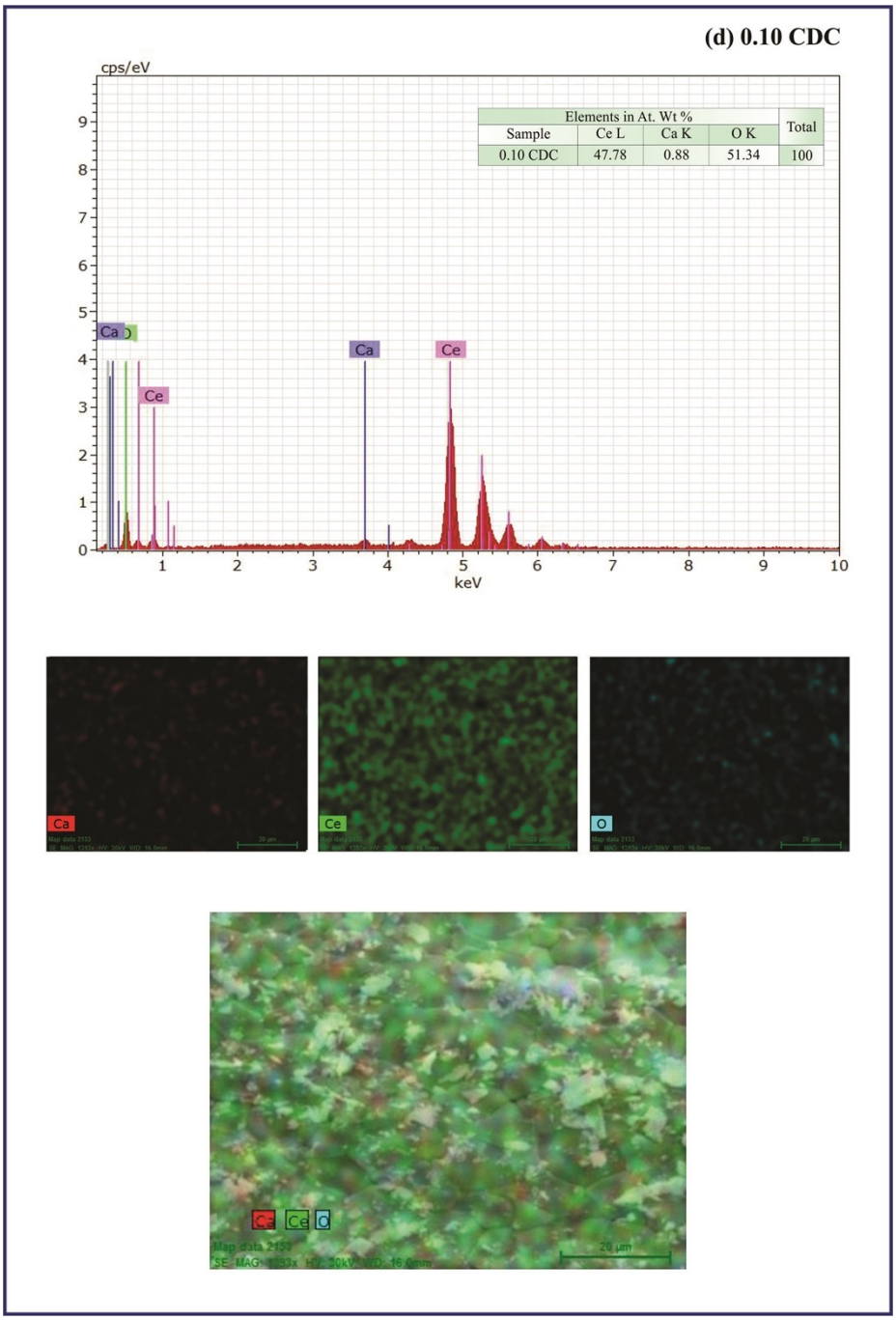

Fig. 5S EDX spectra and elemental mapping of CDC samples.

References

1 V. Thangadurai, P. Kopp, Chemical synthesis of Ca-doped CeO2-Intermediate temperature oxide ion electrolytes, J. Power Sources, 2007, **168**, 178. https://doi.org/10.1016/j.jpowsour.2007.03.030.

2 R. Murugan, L. Kashinath, R. Subash, P. Sakthivel, K. Byrappa, S. Rajendran, G. Ravi, Pure and alkaline metal ion (Mg, Ca, Sr, Ba) doped cerium oxide nanostructures for photo degradation of methylene blue, Mate. Res. Bull., 2018, **97**, 319. https://doi.org/10.1016/j.materresbull.2017.09.026.

3 R. Suresh, V. Ponnuswamy, R. Mariappan, Effect of annealing temperature on the microstructural, optical and electrical properties of CeO_2 nanoparticles by chemical precipitation method, Appl. Surf. Sci., 2013, **273**, 457. https://doi.org/10.1016/j.apsusc.2013.02.062.

4 S. Samiee, E.K. Goharshadi, Effects of different precursors on size and optical properties of ceria nanoparticles prepared by microwave-assisted method, Mater. Res. Bull., 2012, 47, 1089. https://doi.org/10.1016/j.materresbull.2011.12.058.

5 G. Wang, Q. Mu, T. Chen, Y. Wang, Synthesis, characterization and photoluminescence of CeO_2 nanoparticles by a facile method at room temperature, J. Alloys Compd., 2010, **493**, 202,. https://doi.org/10.1016/j.jallcom.2009.12.053.

6 C. Ho, J.C. Yu, T. Kwong, A.C. Mak, S. Lai, Morphology-controllable synthesis of mesoporous CeO_2 nano and microstructures, Chem. Mater., 2005, **17**, 4514. https://doi.org/10.1021/cm0507967.

7 R. Tholkappiyan, K. Vishista, Synthesis and characterization of barium zinc ferrite nanoparticles: Working electrode for dye sensitized solar cell applications, Sol. Energy, 2014, **106**, 118. https://doi.org/10.1016/j.solener.2014.02.003.

8 T.H. Hsieh, D.T. Ray, Y.P. Fu, Co-precipitation synthesis and AC conductivity behavior of gadolinium-doped ceria, Ceram. Int., 2013, **39**, 7967. https://doi.org/10.1016/j.ceramint.2013.03.061.

9 M. Karl Chinnu, K. Vijai Anand, R. Mohan Kumar, T. Alagesan, R. Jayavel, Synthesis and enhanced electrochemical properties of Sm:CeO_2 nanostructure by hydrothermal route, Mater. Lett., 2013, **113**, 170. https://doi.org/10.1016/j.matlet.2013.09.036.

10 F. Abbas, T. Jan, J. Iqbal, I. Ahmad, M.S.H. Naqvi, M. Malik, Facile synthesis of ferromagnetic Ni doped CeO_2 nanoparticles with enhanced anticancer activity, Appl. Surf. Sci., 2015, **357**, 931. https://doi.org/10.1016/j.apsusc.2015.08.229.